

# Tin hypthiodiphosphate: nonlinear response in the sub-100 fs time domain

M. Imlau,<sup>1,\*</sup> V. Dieckmann,<sup>1</sup> H. Badorreck,<sup>1</sup> and A. Shumelyuk<sup>2</sup>

<sup>1</sup>Department of Physics, University of Osnabrück, Barbarastr. 7, 49069 Osnabrück, Germany

<sup>2</sup>Institute of Physics, National Academy of Sciences, 46, Science Avenue, 03 650 Kyiv, Ukraine

\*[mimlau@uni-osnabrueck.de](mailto:mimlau@uni-osnabrueck.de)

**Abstract:** The interaction of sub-100 fs light pulses ( $\tau_p \lesssim 75$  fs) with single crystals of nominally undoped tin hypthiodiphosphate,  $\text{Sn}_2\text{P}_2\text{S}_6$ , is studied in the near-infrared spectral range (590 – 1630 nm). A predominant contribution of the two-photon absorption (TPA) is verified in the measurements of the sample transmission as a function of pulse intensity and of the time delay between pump and probe pulses. Scans over the photon energy show that the two-photon absorption coefficient  $\beta$  increases in a superlinear way for photon energies  $\hbar\omega$  exceeding  $E_g/2$ ; for any quantum energy it is nearly independent of propagation direction and polarization of the incident beam. Such a behavior is qualitatively similar to that predicted by perturbation theory within models with allowed-forbidden transitions. The TPA coefficient saturates at a maximum value of  $\beta \approx 8 \text{ cm GW}^{-1}$  at  $\hbar\omega \approx 1.80 \text{ eV}$ . It drops when reaching the bandgap  $E_g$ . Using pump-probe measurements at 626 nm, a transient absorption is verified that persists for probe pulse delays much longer than the pump pulse duration, up to 2.5 ns. We discuss our results in the framework of the microscopic structure of  $\text{Sn}_2\text{P}_2\text{S}_6$  with emphasis on the optical generation of  $\text{S}^-$  small hole polarons.

© 2011 Optical Society of America

**OCIS codes:** (160.4670) Optical materials; (190.7110) Ultrafast nonlinear optics; (260.7120) Ultrafast phenomena; (300.6420) Spectroscopy, nonlinear; (300.6530) Spectroscopy, ultrafast.

---

## References and links

1. G. Dittmar and H. Schäfer, "Crystal structure of  $\text{Sn}_2\text{P}_2\text{S}_6$ ," *Z. Naturforsch. B* **29B**, 312–317 (1974).
2. R. V. Gamernyk, Yu. P. Gnatenko, P. M. Bukivsij, P. A. Skubenko, and V. Yu. Slivka, "Optical and photoelectric spectroscopy of photorefractive  $\text{Sn}_2\text{P}_2\text{S}_6$  crystals," *J. Phys.: Condens. Matter* **18**, 5323–5331 (2006).
3. K. Kuepper, B. Schneider, V. Caciuc, M. Neumann, A. V. Postnikov, A. Ruediger, A. A. Grabar, and Yu. M. Vysochanskii, "Electronic structure of  $\text{Sn}_2\text{P}_2\text{S}_6$ ," *Phys. Rev. B* **67**, 115101 (2003).
4. Yu. M. Vysochanskii, K. Glukhov, K. Fedyo, and R. Yevych, "Charge transfer and anharmonicity in  $\text{Sn}_2\text{P}_2\text{S}_6$  ferroelectrics," *Ferroelectrics* **414**, 30–40 (2011).
5. S. G. Odoulov, A. N. Shumelyuk, U. Hellwig, R. A. Rupp, A. A. Grabar, and I. M. Stoyka, "Photorefraction in tin hypthiodiphosphate in the near infrared," *J. Opt. Soc. Am. B* **13**, 2352–2360 (1996).
6. A. A. Grabar, M. Jazbinsek, A. N. Shumelyuk, Yu. M. Vysochanskii, G. Montemezzani, and P. Günter, "Photorefractive effects in  $\text{Sn}_2\text{P}_2\text{S}_6$ ," in *Photorefractive Materials and Their Applications II*, P. Günter and J.-P. Huignard, eds. (Springer Verlag, 2007), pp. 327–362.
7. R. Mosimann, P. Marty, T. Bach, F. Juvalta, M. M. Jazbinsek, P. Günter, A. A. Grabar, I. M. Stoyka, and M. Vysochanskii, "High-speed photorefraction at telecommunication wavelength 1.55  $\mu\text{m}$  in  $\text{Sn}_2\text{P}_2\text{S}_6\text{:Te}$ ," *Opt. Lett.* **32**, 2330–2332 (2007).
8. A. Shumelyuk, A. Hryhorashchuk, and S. Odoulov, "Coherent optical oscillator with periodic zero- $\pi$  phase modulation," *Phys. Rev. A* **72**, 023819 (2005).
9. A. Ruediger, O. Schirmer, S. Odoulov, A. Shumelyuk, and A. Grabar, "Studies of light-induced charge transport in  $\text{Sn}_2\text{P}_2\text{S}_6$  by combined EPR/optical absorption spectroscopy," *Opt. Mater.* **18**, 123–125 (2001).

10. A. Shumelyuk, M. Wesner, M. Imlau, and S. Odoulov, "Double-phase conjugate mirror in nominally undoped  $\text{Sn}_2\text{P}_2\text{S}_6$ ," *Opt. Lett.* **34**, 734–736 (2009).
11. A. Shumelyuk and S. Odoulov, "Light pulse manipulation in  $\text{Sn}_2\text{P}_2\text{S}_6$ ," *J. Opt.* **12**, 104015 (2010).
12. G. von Bally, F. Rickermann, S. Odoulov, and A. Shumelyuk, "Near-infrared holographic recording in  $\text{Sn}_2\text{P}_2\text{S}_6$  with nanosecond pulses," *Phys. Status Solidi A* **157**, 199–204 (1996).
13. T. Bach, K. Nawata, M. Jazbinsek, T. Omatsu, and P. Günter, "Optical phase conjugation of picosecond pulses at  $1.06\ \mu\text{m}$  in  $\text{Sn}_2\text{P}_2\text{S}_6\text{:Te}$  for wavefront correction in high-power Nd-doped amplifier systems," *Opt. Express* **18**, 87–95 (2010).
14. A. A. Grabar, I. V. Kedyk, M. I. Gurzan, I. M. Stoika, A. A. Molnar, and Y. M. Vysochanskii, "Enhanced photorefractive properties of modified  $\text{Sn}_2\text{P}_2\text{S}_6$ ," *Opt. Commun.* **188**, 187–194 (2001).
15. O. Beyer, D. Maxien, K. Buse, B. Sturman, T. H. Hsieh, and D. Psaltis, "Investigation of nonlinear absorption processes with femtosecond light pulses in lithium niobate crystals," *Phys. Rev. E* **71**, 056603 (2005).
16. M. Sheik-Bahae, A. A. Said, T.-H. Wei, D. J. Hagan, and E. W. Van Stryland, "Sensitive measurement of optical nonlinearities using a single beam," *IEEE J. Quantum Electron.* **26**, 760–769 (1990).
17. V. Nathan, A. H. Guenter, and S. S. Mitra, "Review of multiphoton absorption in crystalline solids," *J. Opt. Soc. Am. B* **2**, 294–316 (1985).
18. E. W. Van Stryland, M. A. Woodall, H. Vanherzeele, and M. J. Soileau, "Energy band-gap dependence of two-photon absorption," *Opt. Lett.* **10**, 490–492 (1985).
19. D. C. Hutchings and B. S. Wherrett, "Theory of anisotropy of two-photon absorption in zinc-blende semiconductors," *Phys. Rev. B* **49**, 2418–2426 (1994).
20. A. Ruediger, "Light induced charge transfer processes and pyroelectric luminescence in  $\text{Sn}_2\text{P}_2\text{S}_6$ ," PhD thesis (University of Osnabrück, 2001).
21. D. Berben, K. Buse, S. Wevering, P. Herth, M. Imlau, and T. Woike, "Lifetime of small polarons in iron-doped lithium-niobate crystals," *J. Appl. Phys.* **87**, 1034–1041 (2000).
22. O. F. Schirmer, " $\text{O}^-$  bound small polarons in oxide materials," *J. Phys.: Condens. Matter* **18**, R667–R704 (2006).
23. P. Herth, T. Granzow, D. Schaniel, Th. Woike, M. Imlau, and E. Krätzig, "Evidence for light-induced hole polarons in  $\text{LiNbO}_3$ ," *Phys. Rev. Lett.* **95**, 067404 (2005).
24. S. Torbrügge, M. Imlau, B. Schöke, C. Merschjann, O. F. Schirmer, S. Vernay, A. Gross, V. Wesemann, and D. Rytz, "Optically generated small electron and hole polarons in nominally undoped and Fe-doped  $\text{KNbO}_3$  investigated by transient absorption spectroscopy," *Phys. Rev. B* **78**, 125112 (2008).
25. Y. Qiu, K. B. Ucer, and R. T. Williams, "Formation time of a small electron polaron in  $\text{LiNbO}_3$ : measurements and interpretation," *Phys. Status Solidi C* **2**, 232–235 (2005).

## 1. Introduction

Tin hypophosphite ( $\text{Sn}_2\text{P}_2\text{S}_6$ , SPS) is a low symmetry (monoclinic) ferroelectric-semiconductor crystal ( $Pn$  at room temperature [1]) with a bandgap of 2.35 eV ( $\alpha = 35\ \text{cm}^{-1}$ ) [2]. Its microscopic structure is built from  $\text{Sn}^{2+}$  ions and  $(\text{P}_2\text{S}_6)^{4-}$  clusters with a largely covalent binding character of the P-P and P-S bonds [3]. The energy band structure and charge density distribution has been reported for non-stoichiometric crystals by first-principles in the LDA approach, only recently [4].

SPS provides a remarkable photorefractive nonlinearity at ambient temperatures: The two-beam coupling gain factor exceeds  $20\ \text{cm}^{-1}$  due to its large Pockels coefficient ( $r_{111} \approx 170\ \text{pm V}^{-1}$ ) and an astonishingly short response time in the order of milliseconds is reported in the red-spectral range (632 nm) [5, 6]. For Te-doped SPS, a photorefractive response was verified even at the communication wavelength of  $1.55\ \mu\text{m}$  [7]. Commonly, two types of movable charge carriers of different sign take part in the build-up of space-charge gratings [8] with holes being the dominating carriers [9]. As a result the spectrum of the two-beam coupling gain has a narrow dip at zero frequency detuning. There are several positive consequences of such a behavior. For instance, it is possible to switch from light slowing down to superluminal propagation (or vice versa) by simply changing the input pulse duration [10]. It affects also the temporal dynamics of four-wave mixing coherent oscillators, which may switch to periodic pulses with rapidly changing phase between two discrete values (zero and  $\pi$ ) [11].

So far, the nonlinear response of SPS was widely studied using exposure to continuous wave (cw) laser light. Also, the aspect of exposure to laser pulses with nanosecond [12] or picosecond [13] pulse durations was treated in the framework of near-infrared holographic recording

and optical phase conjugation. This revealed a nonlinear response similar to the cw-experiments if referenced to the mean intensity. Taking a further increase of the peak pulse power in the context of wave-mixing phenomena in SPS into account, one might expect to enable nonlinearities that are different from photorefraction and that decay with much shorter relaxation times (below  $\mu\text{s}$ ). The purpose of this work is to study the nonlinear response of nominally undoped SPS exposed to ultra-short laser pulses with pulse duration of 75 fs, pulse intensities up to  $1.5 \text{ PW m}^{-2}$  and over a wide spectral range in the red and near-infrared spectral range from 590 nm till 1600 nm, i.e., for photon energies below the bandgap energy.

## 2. Experimental procedure

Two sets of experiments are described in this paper. The first one aims to measure the transmission changes of the sample as a function of the incident pulse intensity. The second one allows for probing the light-induced transients during and after the pulse in the time domain up to 2.5 ns using a pump-probe technique.

For the transmission studies, the pulse intensity was varied by using neutral density (ND) filters (Fig. 1a) with  $f(L1) = 350 \text{ mm}$ . The transmission was obtained from the energy ratio of transmitted and incoming beams detected using Si-PIN photodiodes D1 and D3 (Thorlabs DET10A). For this purpose, thin lenses with focal lengths of 35 mm were used to adjust the spatial beam profile to the narrow aperture of the photodiodes (sensitive area of  $A = 0.8 \text{ mm}^2$ ).

The set-up for the pump-probe experiment is sketched schematically in Fig. 1b). Pump and probe beams are slightly focused by concave mirrors KM1 and KM2 ( $r = 1 \text{ m}$ ) to the SPS sample with an intersection angle of  $\approx 4.6^\circ$  measured in air. The incident pulse energies are detected by the diodes D3 and D4 via a glass plate placed in front of the SPS sample. The temporal delay between pump and probe pulses is adjusted from  $-0.8 \text{ ns}$  to  $2.5 \text{ ns}$  by an optical delay line (DL) in steps of 8.3 fs. Both beams, attenuated if necessary by neutral density filters ND1 and ND2 are chopped by a phase-synchronized chopper wheel to less than 3 Hz. Thus, any effect of the previous pump pulse on the actual measurement is suppressed and the thermal load of the sample is reduced.

The ratio of the probe beam signals collected from D1 and D3, proportional to the samples' transmission, is taken to be unity for zero intensity of the pump pulse. In such a way all intensity independent losses (for relatively small linear absorption and for Fresnel reflection from the sample faces) are eliminated from the measured transmittance to ensure the easy extraction of the nonlinear absorption coefficient. (The linear absorption coefficient will be taken into account in what follows, however, when estimating the effective interaction length inside the sample.)

Femtosecond pulses in the spectral range of 600 nm to 1600 nm are generated in two optical parametric amplifiers (Coherent Inc., *OPerA solo*) pumped by a regeneratively amplified  $\text{Ti}^{3+}:\text{Al}_2\text{O}_3$  oscillator (Coherent Inc., *Libra-F HE*) at  $\lambda = 802 \text{ nm}$  with a repetition rate of 1 kHz. At the sample, pulse energies in the order of  $100 \mu\text{J}$  are available with pulse durations of  $\lesssim 75 \text{ fs}$  (Gaussian shape approximation, determined using interferometric auto correlation, APE Angewandte Physik und Elektronik GmbH, *Pulse Check PD 15ps*). The spatial intensity distribution of the light beam is close to a Gaussian profile and nearly axially symmetric. Thus, it can be expressed via:

$$I_p(x=0) = I_p^0 \exp[-(t/t_p)^2 - (r/r_p)^2] \quad . \quad (1)$$

Here,  $I_p^0$  is the input pulse peak intensity,  $t_p$  and  $r_p$  represent pulse duration and beam radius, respectively.

Our study was performed with nominally undoped SPS samples grown in the Institute of Solid State Physics and Chemistry of Uzhgorod State University by chemical vapor transport.

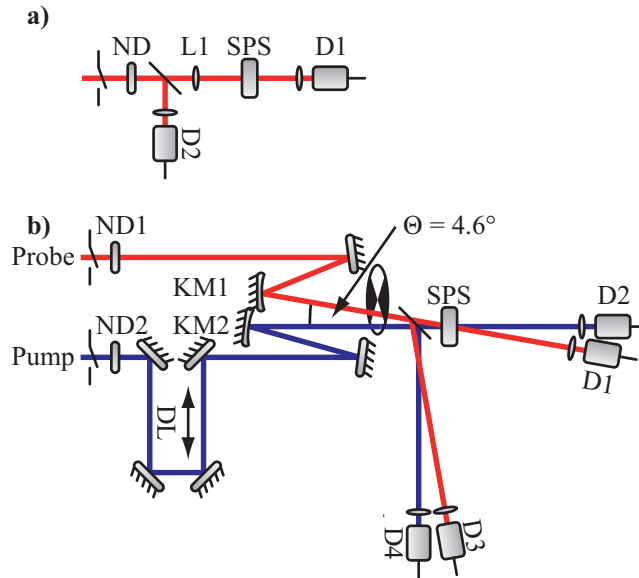


Fig. 1. Schematic representation of the experimental set-ups. a) Single beam set-up for determination of the nonlinear absorption. The beam is attenuated by ND-filters and slightly focused by lens L1 to the sample. b) Pump-probe setup: both beams, attenuated by ND-filters, are focused to the sample by concave mirrors KM1, KM2. The pump beam is delayed in the time domain by the delay line DL.

Iodine was used as transport gas. The samples are of good optical quality and were classified to type I by measurements of the kinetics of the beam-coupling gain [6, 14]. The rectangular sample of nominally undoped SPS (sample identifier: *N159*) used for determination of the two-photon absorption (TPA) coefficient measures  $5.6 \times 6.2 \times 3.5 \text{ mm}^3$  along the crystallographic axes  $x$ ,  $y$ , and  $z$ , respectively, and its  $z$  faces are optically finished. The measurements of the TPA anisotropy were performed with a sample where all faces have been optically finished *K4* ( $8.0 \times 8.0 \times 8.0 \text{ mm}^3$ ). Pump-probe experiments were performed in a thick sample *K16* ( $10.0 \times 8.5 \times 6.5 \text{ mm}^3$ ) that allows for a better signal-to-noise ratio.

### 3. Experimental results and discussion

#### 3.1. Single beam two-photon absorption

The left frame of Fig. 2 represents the reciprocal transmission  $T^{-1}$  as a function of intensity. The data are depicted for the case of beam propagation along the  $z$ -direction for several selected wavelengths in the range from  $E_g/2$  to  $E_g$ .

A noticeable beam attenuation of more than one order of magnitude is clearly observed. It can obviously be assigned to nonlinear absorption, because no pronounced photoinduced scattering or new light beams are detected during the measurements. We'd like to note, that supplementary investigations using the  $z$ -scan technique in principle allow the simultaneous detection of possible nonlinear refractive-index changes induced by the fs pulse. This aspect will be dealt with in the frame of another experimental study.

It is reasonable to assume that the observed beam attenuation is due to two-photon absorption (TPA). This is very likely, because of the photon energies being in a range below the bandgap energy, and particularly covering  $E_g/2$ . Further, TPA of sub-ps-pulses has already been reported for other wide bandgap ferroelectric photorefractive crystals like  $\text{LiNbO}_3$  [15], as well.

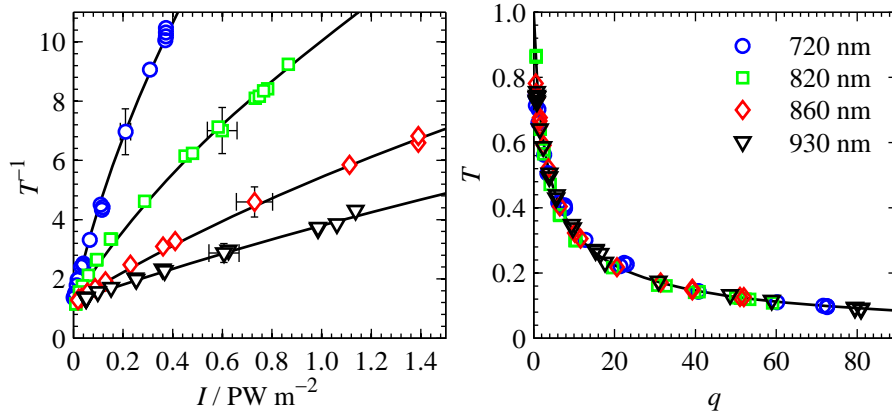


Fig. 2. Reciprocal transmittance of the 3.5 mm thick SPS sample versus maximum peak on-axis intensity  $I_p^0$  of the 73 fs pulse on the input face (left frame), and sample transmission versus dimensionless parameter  $q = \beta I_p^0 \ell$  (right frame). The light beam propagates along the  $z$ -axis and is polarized along the  $x$ -axis. Circles, squares, diamonds, and triangles mark the wavelengths of the incident pulse as indicated in the legend. The solid lines in the left frame serve to guide the eye, while in the right frame it represents the dependence calculated for solely two-photon absorption (see Eq. (2)).

For proving this hypothesis, we model the transmission  $T$  as a function of the dimensionless parameter  $q = \beta I_p^0 \ell$  according to Ref. [16]. Here,  $\ell$  is the *effective* sample thickness that takes into account beam extinction due to linear absorption,  $I_p^0$  is the intensity of the incident beam and  $\beta$  is the two-photon absorption coefficient. For the particular case of two-photon absorption, and with the assumption of a laser pulse with spatial and temporal Gaussian shapes,  $T(q)$  can be expressed by:

$$T(q) = \frac{2}{q\sqrt{\pi}} \int_0^\infty \ln [1 + q \exp(-s^2)] ds. \quad (2)$$

Provided  $\ell$  and the peak power of the incident beam  $I_p^0$  are determined,  $\beta$  remains as single free parameter for plotting  $T_{\text{exp}}(q)$  using the experimentally determined transmission values. Optimizing the accordance of  $T_{\text{exp}}(q)$  and  $T(q)$ , we obtain the material parameter  $\beta$ . The fitting procedure is performed by minimizing

$$\chi_R^2(\beta) = \sum_i \frac{[T_{\text{exp}}(q_i) - T(q_i)]^2}{T(q_i)}, \quad (3)$$

i.e., the normalized quadratic deviation of the measured data from the fitting curve at a specific value of  $q$ . The outcome of the fitting procedure is depicted in Fig. 2 (right frame). Here, we have determined the effective sample thickness from the coefficients of the linear absorption and the sample dimension in  $z$ -direction. The incident beam intensity was calculated from Eq. (1) with the energy of the pulse entering the crystal, the beam waist and the pulse duration  $2t_p = \tau_p / \sqrt{\ln 2}$ , with  $\tau_p = 73$  fs being the FWHM of the pulse. Losses for Fresnel reflection from the input face are taken into account. Obviously, an excellent agreement between  $T_{\text{exp}}(q)$  and  $T(q)$  can be obtained, thus supporting the validity of TPA-model approach.

This procedure has been performed over the spectral range of 590 nm to 1630 nm so that we obtained the dispersion of  $\beta(\hbar\omega)$  depicted in Fig. 3.

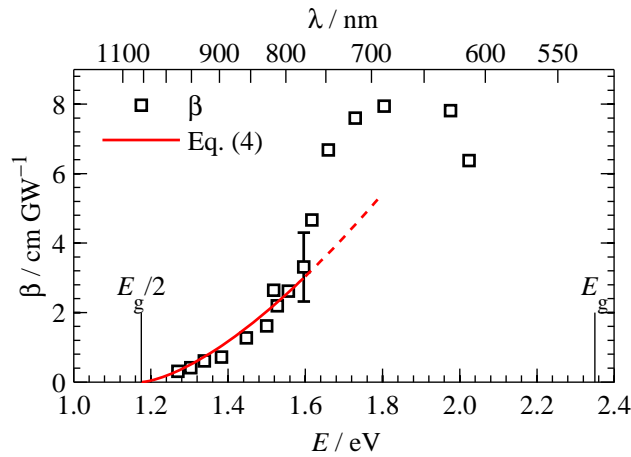


Fig. 3. Photon energy  $E = \hbar\omega$  dependence of the TPA coefficient  $\beta$  of nominally undoped SPS. The light beam propagates along the  $z$ -axis and is polarized along the  $x$ -axis. The red solid line shows the result of the fit of Eq. (4) to the experimental data in the range of  $E_g/2$  to 1.6 eV. The dashed part (from 1.6 to 1.8 eV) is a continuation of the function using the parameters obtained from the fitting procedure.

The TPA nearly vanishes below  $\hbar\omega = 1.2$  eV, i.e., when the energy of two photons is near to or lower than the bandgap of SPS (at ambient temperature  $E_g \simeq 2.35$  eV according to Ref. [2]). For photon energies ranging from  $E_g/2$  to 1.6 eV the TPA coefficient follows the functional dependence:

$$\beta \propto \left[ \left( \frac{2\hbar\omega}{E_g} \right) - 1 \right]^{3/2}. \quad (4)$$

In the range of  $1.6 \text{ eV} < \hbar\omega < 1.7 \text{ eV}$ , a pronounced increase of  $\beta$  is found, while it saturates at  $\approx 1.8$  eV. This increase can not be modeled by Eq. (4) that is plotted for comparison in the range from 1.6 to 1.8 eV using the parameters obtained from the fitting procedure (dotted part of the red line in Fig. 3). For photon energies  $\hbar\omega \geq 2.0$  eV, the TPA coefficient decreases. Similar behavior on the photon energy is found for different light polarizations and directions of beam propagation with respect to the crystallographic axes. Slightly smaller values (within 10%) of  $\beta$  were measured solely for a beam propagating along the  $z$ -axis as compared to the two other directions.

In perturbation theories of two-photon absorption the characteristic superlinear photon energy dependence of  $\beta$  according to Eq. (4) is usually an issue of models with allowed-forbidden transitions [17–19]. As it is shown in Ref. [19] the TPA coefficient follows the dependence of Eq. (4) starting from  $\hbar\omega$  very close to  $E_g/2$ , but then tends to saturation for higher quantum energies. Thus, at least in the range of  $\hbar\omega$  from 1.2 to 1.6 eV the TPA coefficient features one of the two known standard behaviors. However, more careful theoretical analysis is necessary.

For the analysis of the characteristic behavior of  $\beta(\hbar\omega)$  for quantum energies exceeding 1.6 eV, we consider the results obtained with combined EPR/absorption spectroscopy [9]. Very strong light-induced changes of the absorption were found in nominally undoped samples. Predominant is the appearance of a broad absorption feature with a maximum at 2.0 eV and a band width of  $\approx 0.8$  eV [9, 20]. As will be described below, this photochromism can be related to the formation of  $S^-$  small hole polarons [4]. It is reasonable to suggest the possibility that the populated energy levels give rise to single-photon absorption in this spectral region as well,

which will affect the two-photon absorption. However, a compelling precondition is that the formation time of the light-induced absorption falls within the duration of the pump pulse, i.e. below 75 fs.

It should be mentioned that nonlinear absorption was also observed for photon energies below  $E_g/2$ . However, the beam attenuation was comparatively weak in this spectral range. Furthermore, its intensity dependence strongly deviated from the behavior shown in Fig. 2 (left frame), i.e., the transmission decreased more rapidly as a function of intensity. It is reasonable to attribute this effect to three-photon absorption.

### 3.2. Pump-probe experiments

Figure 4 shows the dependence of the probe beam transmission on the temporal delay  $\Delta t$  between pump and probe pulses up to  $\Delta t = 25$  ps. The results are depicted for a probe beam propagation along the  $z$ -axis of the sample, a light polarization parallel to the  $y$ -axis, and identical wavelengths of  $\lambda = 626$  nm (1.98 eV) for pump and probe pulse. Their respective intensities are set to  $(860 \pm 50)$  TW m<sup>-2</sup> and  $(4.6 \pm 0.3)$  TW m<sup>-2</sup>, i.e., an intensity ratio of  $\approx 190 : 1$ . At 626 nm, the linear absorption was determined to  $\alpha = (0.49 \pm 0.05)$  cm<sup>-1</sup>.

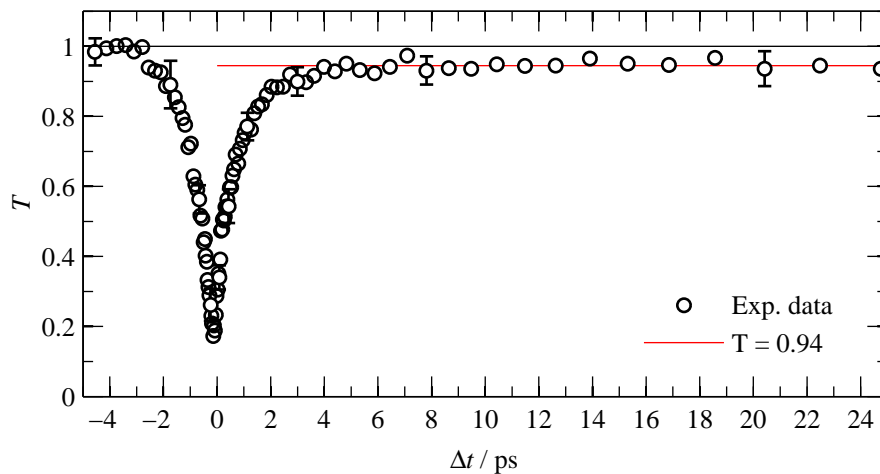


Fig. 4. Beam attenuation of the SPS sample *K16* as a function of the time delay between pump and probe pulses. Wavelength:  $\lambda = 626$  nm, light polarization parallel  $y$ -axis, and beam propagation along  $z$ -direction. The red line marks the saturation value of the transmission of  $T \approx (94 \pm 2)\%$  for  $\Delta t \gg 5$  ps.

The normalized transmission shows a strong decrease to a value below 20% as compared to the transmission of the unexposed sample, i.e., to the transmission for  $\Delta t \rightarrow -\infty$ . The value of the transmission in the minimum depends on the pulse intensity in accordance with our findings in the previous section (Fig. 2, left frame), so that we can attribute this dip to the presence of two-photon absorption. Therefore, the delay time, at which the minimum value of  $T(\Delta t)$  is observed, corresponds to the superposition of pump and probe pulses in the time domain ( $\Delta t = 0$ ).

For probe pulse delays  $\Delta t \gg \tau_p$  (shown up to 25 ps after the pump pulse in the figure), the transmission value remains constant at  $T = (94 \pm 2)\%$  (red line). Hence, the initial value related to the presence of linear absorption is not recovered. This transmission value was still observed for the maximum time delay of  $\Delta t = 2.5$  ns that can be adjusted with our experimental setup. Probing the sample transmission with one of the subsequent probe pulses at  $\Delta t = 1$  s, the initial

transmission  $T(\Delta t \rightarrow -\infty)$  was measured. According to this signal recovery we conclude the presence of a transient absorption induced by the pump pulse. This signal can not be assigned to pump-pulse induced damages to the sample's surface or bulk. Influences of the transient absorption induced by the previous pump pulse are eliminated by reducing the repetition rate of our measurement to less than 3 Hz.

Such transients are reported for a variety of ferroelectric semiconductors upon exposure to ns- and fs-laser pulses. The effect can be either attributed to free-carrier absorption or to absorption that is due to formation of small polarons. Respective optically generated carrier densities decay with relaxation times in the range from several tens of picoseconds up to milliseconds (free carriers) and seconds (small bound polarons). For instance, the transients in ferroelectric  $\text{LiNbO}_3$ , where small polaron formation is confirmed (e.g.  $\text{Nb}_{\text{Li}}^{4+}$  in Ref. [21]), show relaxation times in the range of a few milliseconds (see Ref. [15]).

For non-stoichiometric nominally undoped SPS, the optical formation of  $\text{S}^-$  small hole polarons seems likely in accordance with the recent results of Vysochanskii et al. [4]: Light exposure removes electrons from the valence band, that is formed by 3p orbitals from sulfur and phosphorous. Thus, the remaining hole recharges  $\text{S}^{2-}$  yielding  $\text{S}^-$  that is related with a structural deformation, i.e. small hole polarons [22] appear. The optical features of  $\text{S}^-$  were shown to coincide with the light-induced broad absorption feature at 2.0 eV [4] that were experimentally reported by Ruediger et al. [9].

Taking these aspects into account, we can suggest the following mechanism for the appearance of the transients at 626 nm: The pump pulse (1.98 eV) generates a significant density of  $\text{S}^-$  small hole polarons by removing electrons from the valence band via two-photon absorption. The probe pulse (1.98 eV) is attenuated due to the broad absorption feature of the  $\text{S}^-$  absorption band that is centered at 2.0 eV. The subsequent relaxation of the induced polaron density may occur via hopping of thermally activated polarons between different  $\text{S}^{2-}$  sites with the ultimate electron-hole recombination in the time domain less than one second. It should be noted that similar processes initiated by two-photon absorption were reported upon ns-laser pulse exposure in various nominally undoped ferroelectrics such as  $\text{LiNbO}_3$  and  $\text{KNbO}_3$  [23, 24]. It is likely, that hole polaron formation appears in the temporal range below 200 fs, as it was experimentally studied in the original work of Qiu et al. for small polarons in  $\text{LiNbO}_3$  [25]. Thus, the formation is overlaid by the strong beam attenuation related to two-photon-absorption and can not be resolved in our experiment. Measurements of the temperature dependence of the relaxation time and with different photon energies of pump- and probe pulses are necessary to verify this model approach for SPS.

#### 4. Conclusion

Femtosecond pulses with photon energies within the range from 0.76 eV to 2.1 eV are strongly attenuated when propagating through the SPS sample because of instantaneous nonlinear absorption via two-photon or three-photon absorption. The measured TPA coefficients  $\beta$  up to  $8 \text{ cm GW}^{-1}$  are by a factor of two higher than the values reported for other wide bandgap ferroelectrics, such as  $\text{LiNbO}_3$  [15], while being lower in comparison to semiconductor crystals [18]. A second feature of fs-pulse interaction with SPS is the appearance of a metastable transient absorption that is typical for a variety of wide bandgap ferroelectrics. It might be attributed to the optical generation of  $\text{S}^-$  small hole polarons.

#### Acknowledgements

The financial support of the Deutsche Forschungsgemeinschaft via projects IM 37/5-1, IM 37/7-1, and INST 190/137-1 FUGG is gratefully acknowledged. We are thankful to A. Grabar and I. Stoyka for SPS samples and to S. Odoulov for helpful discussions. A. Shumelyuk is



grateful to the German colleagues for their hospitality during his stay in Osnabrück as DFG guest scientist.